PROCEEDINGS OF SCIENCE

Beam normal single-spin asymmetry in electron-proton scattering with intermediate state resonances

Jaseer Ahmed,[a] **Peter Blunden**[b,*] **and Wally Melnitchouk**[c]

[a] *Department of Physics, Shahjalal University of Science and Technology, Sylhet-3114, Bangladesh*

[b] *Department of Physics and Astronomy, University of Manitoba, Winnipeg, MB R3T 2N2, Canada*

[c] *Jefferson Lab, Newport News, VA 23606, USA*

E-mail: jaseer-phy@sust.edu, blunden@physics.umanitoba.ca, wmelnitc@jlab.org

This contribution highlights results from our recent calculations of beam normal single-spin asymmetries in electron–proton elastic scattering that depend on the imaginary (absorptive) part of two-photon exchange amplitudes. The intermediate hadronic states are modelled by spin 1/2 and 3/2 resonance states below 1.8 GeV in mass. CLAS exclusive meson electroproduction data are used as input for the transition amplitudes from the proton to the resonance states, and we also include the effect of resonance widths. We compare results with data from the SAMPLE, A4, and Qweak experiments.

25th International Spin Physics Symposium (SPIN 2023)
24-29 September 2023
Durham, NC, USA

[*] Speaker

PoS(SPIN2023)179

1. Introduction

Over the last two decades the role of two-photon exchange (TPE) in electron–proton elastic scattering has received considerable attention, in both the theoretical and experimental nuclear physics communities, in an effort to understand its impact on hadron structure dependent observables [1–4]. Among these is the analysis of the proton's electric (G_E) to magnetic (G_M) form factor ratio, $\mu_p G_E/G_M$, where μ_p is the proton's magnetic moment, and the well-known discrepancy between determinations of this ratio by the longitudinal-transverse (LT) separation and the polarization transfer (PT) methods. It has been realized for some time now that TPE effects can make large contributions to the former, while having a minimal effect on the latter [5–7].

The use of hadronic degrees of freedom to calculate the TPE amplitude $\mathcal{M}_{\gamma\gamma}$ can be considered as a reasonable approximation for low to moderate values of four-momentum transfer, $Q^2 \lesssim 5\ \mathrm{GeV}^2$, where hadrons are expected to retain their identity. In our recent work [8], we follow the dispersive approach for resonant intermediate state contributions to $\mathcal{M}_{\gamma\gamma}$ developed in Ref. [9]. On-shell form factors are used explicitly to calculate the imaginary part of $\mathcal{M}_{\gamma\gamma}$ from unitarity, with the real (dispersive) part then obtained from a dispersion integral. We account for nine spin-$1/2^{\pm}$ and spin-$3/2^{\pm}$ resonances with mass below 1.8 GeV, and allow for a finite Breit-Wigner width for each individual resonance. In our numerical calculations, for the resonance electrocouplings at the hadronic vertices we use helicity amplitudes extracted from the analysis of CLAS electroproduction data [10–12]. The model calculation is successful in quantitatively reconciling the discrepancy in the form factor ratio $\mu_p G_E/G_M$ without introducing any significant nonlinearities in ε in the reduced cross section [8].

While the real (dispersive) part of $\mathcal{M}_{\gamma\gamma}$ can be accessed directly from the measurement of the ratio of the unpolarized e^+p to e^-p scattering cross sections, the imaginary (absorptive) part of $\mathcal{M}_{\gamma\gamma}$ can be determined from beam and target normal single-spin asymmetries, denoted B_n and A_n, respectively. TPE generates a single-spin asymmetry (SSA) at leading order in the electromagnetic coupling α, with either the beam or target polarized normal (or transverse) to the scattering plane. Explicitly, the experimentally measured asymmetry is defined by

$$\mathrm{SSA} = \frac{\sigma^{\uparrow} - \sigma^{\downarrow}}{\sigma^{\uparrow} + \sigma^{\downarrow}}, \tag{1}$$

where $\sigma^{\uparrow}$ ($\sigma^{\downarrow}$) is the cross section for ep elastic scattering with either beam or target spin polarized parallel (antiparallel) to the scattering plane defined by the incoming and outgoing electron momenta.

It was first shown by de Rújula *et al.* [13] that time-reversal invariance implies no contribution to SSA from the one-photon exchange (OPE) transition amplitude $\mathcal{M}_{\gamma}$. The leading term of the beam or target normal SSA arises from the absorptive part of the TPE transition amplitude $\mathcal{M}_{\gamma\gamma}$, denoted Abs $[\mathcal{M}_{\gamma\gamma}]$, according to the relation

$$\mathrm{SSA} = \frac{\mathrm{Im}\left(\sum_{\mathrm{spins}} \mathcal{M}_{\gamma}^{*}\,\mathrm{Abs}\,[\mathcal{M}_{\gamma\gamma}]\right)}{\sum_{\mathrm{spins}} |\mathcal{M}_{\gamma}|^2}. \tag{2}$$

As defined in Eq. (2), the SSA is of order α. The beam normal asymmetry B_n is further suppressed by the small factor m_e/E_{lab}, where m_e is the electron mass and E_{lab} is the beam energy in the laboratory frame, so that B_n is expected to be of order $10^{-6}-10^{-5}$ for beam energies in the GeV range. For the target normal SSA A_n there is no additional suppression, and hence it is anticipated to be of order $10^{-3}-10^{-2}$ for the same beam energy. In contrast to B_n, for A_n there are currently no available data for a proton target.

The beam normal SSA B_n plays a particularly important role in parity-violating electron scattering experiments that use longitudinally polarized lepton beams to measure the asymmetry due to the spin flip. As a nonzero B_n could contribute to a false asymmetry, parity-violating experiments typically determine the beam normal SSA as a by-product of the longitudinal parity-violating asymmetry. Several parity-violating experiments [14–21] have determined the beam normal SSA over a range of scattering angles and energies. To better understand the beam SSAs originating from the spin-parity $1/2^{\pm}$ and $3/2^{\pm}$ resonance intermediate states, we revisit our earlier TPE calculation [8] to see how well the resonance model fares for SSA observables. More complete results are given in Ref. [22], including those for target normal SSAs.

2. Beam normal single-spin asymmetries in elastic scattering

For the elastic scattering process $e(k) + N(p) \to e(k') + N(p')$ (see Fig. 1), the four-momenta of the initial and final electrons (with mass m_e) are labelled by k and k', with corresponding lab frame energies $E_{\rm lab}$ and $E'_{\rm lab}$. The initial and final nucleons (mass M) have four-momenta p and p', respectively. The four-momentum transfer from the electron to the nucleon is given by $q = p' - p = k - k'$, with the photon virtuality $Q^2 \equiv -q^2 > 0$. For the TPE process, the two virtual photons transfer four-momenta q_1 and q_2 to the proton, so that $q = q_1 + q_2$.

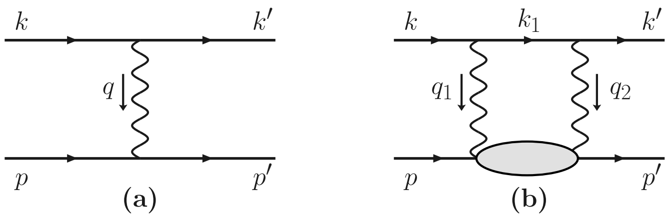

Figure 1: Contributions to elastic electron–nucleon scattering from (a) one-photon exchange (OPE), and (b) two-photon exchange amplitudes, with particle momenta as indicated. The intermediate hadronic state is taken to be a resonance of invariant mass W. The two virtual photons carry momenta q_1 and q_2, giving the total momentum transfer $q = q_1 + q_2$.

For the OPE amplitude the electron mass can be neglected at the kinematics of interest. However, for the B_n SSA the electron mass must be retained for two reasons. First, B_n has an overall factor of m_e, and second, B_n has a mass-dependent quasi-singularity when the intermediate electron three-momentum $|\boldsymbol{k}_1| \to 0$. It is convenient to use the Mandelstam variable s, which is given in the lab frame as $s = M^2 + m_e^2 + 2ME_{\rm lab}$.

For inelastic excitations the minimum value of W is taken to be the pion production threshold, $W_{\rm th} = M + m_\pi$. For a given s, the maximum value of W corresponds to an intermediate electron at rest, $|\boldsymbol{k}_1| = 0$, so that

$$W_{\rm max} = \sqrt{s} - m_e, \qquad E_{k_1} = m_e. \tag{3}$$

At $W = W_{\max}$ the four-momentum transfers of the two virtual photons become

$$Q_1^2 \;=\; Q_2^2 \;=\; m_e \,\frac{(W_{\max}^2 - M^2)}{\sqrt{s}}, \tag{4}$$

so that the two photons are almost on-shell (*i.e.* real). This has been dubbed the quasi-real Compton scattering (QRCS) region [23–26], and requires special attention to reliably compute the SSA numerically.

In the definition of the beam normal SSA in Eq. (2), the denominator is identical to the Born cross section for unpolarized elastic ep scattering, since the spin components have no impact at the Born level. Summing over final state spins and averaging over initial state spins, one can write the squared Born amplitude in terms of the invariant Mandelstam variables s and $Q^2 = -t$,

$$\sum_{\text{spins}} \left|\mathcal{M}_\gamma\right|^2 = \sum_{\text{spins}} \mathcal{M}_\gamma^\dagger \mathcal{M}_\gamma = \frac{e^4}{Q^4}\, D(s, Q^2). \tag{5}$$

The absorptive part of the TPE amplitude in Eq. (2) can be written as

$$\text{Abs}\, \mathcal{M}_{\gamma\gamma} = e^4 \int \frac{d^3 \boldsymbol{k}_1}{(2\pi)^3 2E_{k_1}} \frac{\bar{u}_e(k')\gamma_\mu(\not{k}_1 + m_e)\gamma_\nu u_e(k)}{Q_1^2\, Q_2^2}\, \mathcal{W}^{\mu\nu}. \tag{6}$$

The hadronic tensor $\mathcal{W}^{\mu\nu}$ in Eq. (6) contains all the information about the transition from the proton initial state to all possible intermediate hadronic states, including the elastic nucleon state and the inelastic transitions to the nucleon excited state resonances. In our model, the SSAs are calculated including contributions from each of the spin 1/2 and 3/2 resonance intermediate states below mass $M_R = 1.8$ GeV, which are then added together with the elastic nucleon contribution to obtain the complete result.

Taking the spin sum, one can express the SSA in a concise form in terms of the leptonic and hadronic tensors, $L_{\rho\mu\nu}$ and $H^{\rho\mu\nu}$, respectively, as

$$\text{SSA} = \frac{\alpha Q^2}{\pi D(s, Q^2)} \int \frac{d^3 \boldsymbol{k}_1}{2E_{k_1}} \frac{\text{Im}\, L_{\rho\mu\nu} H^{\rho\mu\nu}}{Q_1^2\, Q_2^2}. \tag{7}$$

For the beam polarized parallel or antiparallel to the normal $\boldsymbol{s}_n$ to the scattering plane the leptonic tensor $L_{\rho\mu\nu}$ contains the lepton polarization vector $s_n^\mu \equiv (0; \boldsymbol{s}_n)$, and takes the form

$$L^{\text{B}}_{\rho\mu\nu} = \frac{1}{2}\, \text{Tr}\left[(1 + \gamma_5 \not{s}_n)(\not{k} + m_e)\gamma_\rho(\not{k}' + m_e)\gamma_\mu(\not{k}_1 + m_e)\gamma_\nu\right], \tag{8}$$

where the superscript "B" denotes the fact that the lepton tensor corresponds to the beam normal case. Note that the imaginary part in Eq. (2) for B_n comes solely from this spin polarization-dependent term. However, the corresponding hadronic tensor for the beam normal case, $H_{\text{B}}^{\rho\mu\nu}$, remains independent of the polarization of the target hadron, and is equivalent to the hadronic tensor for the case of unpolarized ep scattering. We refer the reader to Ref. [22] for details on the hadronic tensor $H_{\text{B}}^{\rho\mu\nu}$.

For the numerical calculation, it will be convenient to transform the phase space integral over the intermediate electron momentum $\boldsymbol{k}_1$ of Eq. (7) in terms of the Lorentz-invariant Mandelstam variable s. Defining the kinematics in the CM frame, the integration over $\mathrm{d}^3\boldsymbol{k}_1 \to \boldsymbol{k}_1^2\,\mathrm{d}|\boldsymbol{k}_1|\,\mathrm{d}\Omega_{k_1}$ can be written as

$$\int \frac{\mathrm{d}^3\boldsymbol{k}_1}{2E_{k_1}} \to -\int_{M^2}^{W_{\max}^2} \mathrm{d}W^2\, \frac{|\boldsymbol{k}_1|}{4\sqrt{s}} \int \mathrm{d}\Omega_{k_1}, \tag{9}$$

with $W_{\max} = \sqrt{s} - m_e$. Thus

$$\mathrm{SSA} = -\frac{\alpha Q^2}{\pi D(s,Q^2)} \int_{M^2}^{W_{\max}^2} \mathrm{d}W^2\, \frac{|\boldsymbol{k}_1|}{4\sqrt{s}} \int \mathrm{d}\Omega_{k_1}\, \frac{\mathrm{Im}\, L_{\rho\mu\nu}H^{\rho\mu\nu}}{Q_1^2 Q_2^2}. \tag{10}$$

The beam normal SSA B_n is sensitive to the quasi-singular behavior of the integrand in Eq. (10) when the intermediate state electron three-momentum $|\boldsymbol{k}_1| \to 0$. This is the QRCS region, where $W \to W_{\max}$ and the two virtual photons have four-momenta Q_1^2 and Q_2^2 of order m_e (see Eq. (4)). In this region of W, the integrand of Eq. (10) is characterized by a slowly varying numerator and a rapidly varying denominator.

To address this behavior in the numerical calculations in a practical way, we evaluate the slowly varying numerator of the integrand in Eq. (10) at $Q_1^2 = Q_2^2 = 0$, which is then a constant independent of θ_{k_1} and ϕ_{k_1}. We keep the mild W dependence, but make no further approximation and leave the denominator intact. Thus we are left with an integral over W in this region that is proportional to the angular integral

$$\frac{|\boldsymbol{k}_1|}{4\sqrt{s}} \int \mathrm{d}\Omega_{k_1}\, \frac{1}{Q_1^2 Q_2^2}. \tag{11}$$

This integral can be done analytically, as discussed in Refs. [9, 23, 26]. We only apply the analytic expression using Eq. (11) to the tail region, $W_{\max} - 5m_e \le W \le W_{\max}$, and use the full three-dimensional numerical quadrature of Eq. (10) elsewhere.

3. Numerical results

In our numerical calculations, for the proton elastic electric (G_E) and magnetic (G_M) form factors we use the parametrization from Ref. [27], which accounts for TPE effects in their extraction. For the hadronic transition currents used in the hadronic tensors $H^{\rho\mu\nu}$ in Eq. (10), we use the CLAS parametrization [12] of the input resonance electrocouplings $A_h(Q^2)$ at the resonance points, where A_h represents the longitudinal electrocoupling, $S_{1/2}$, and the two transverse electrocouplings, $A_{1/2}$ and $A_{3/2}$. The dependence of the electrocouplings A_h on the invariant mass W is given in Ref. [8].

For the inelastic intermediate states in Fig. 1(b) we include the contributions of four spin-parity $3/2^\pm$ resonances $\{\Delta(1232)\,3/2^+$, $N(1520)\,3/2^-$, $\Delta(1700)\,3/2^-$, and $N(1720)\,3/2^+\}$, and five spin-parity $1/2^\pm$ resonances $\{N(1440)\,1/2^+$, $N(1535)\,1/2^-$, $\Delta(1620)\,1/2^-$, $N(1650)\,1/2^-$, and $N(1710)\,1/2^+\}$. The Breit-Wigner mass M_R and the constant decay width Γ_R of the nine excited state resonances are set to those used in the CLAS parametrization [12] of the resonance electrocouplings A_h. We propagate the uncertainty on the input resonance electrocouplings ΔA_h into the estimation of the uncertainties on B_n.

To analyze the role of the resonances on the total SSA, Fig. 2 illustrates the contributions to B_n from the individual resonances at two representative beam energies E_{lab} equal to 0.855 GeV and 3.031 GeV as a function of the laboratory scattering angle θ_{lab}.

PoS(SPIN2023)179

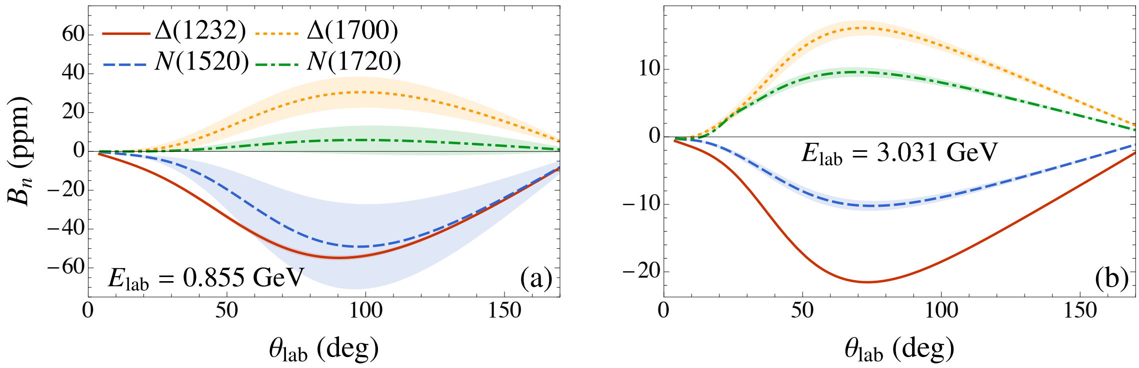

Figure 2: Resonance contributions to the beam normal SSA B_n (in parts per million) as a function of scattering angle $\theta_{\rm lab}$ at two representative beam energies $E_{\rm lab}$ equal to (a) 0.855 GeV and (b) 3.031 GeV. Only the four largest resonance contributors are shown, with the bands reflecting the uncertainties arising from the input electrocouplings.

Among the resonances considered, the four spin-3/2 states $\Delta(1232)$, $N(1520)$, $\Delta(1700)$, and $N(1720)$ have sizeable effects, with some partial cancellation observed between them. Contributions from resonances with spin 1/2 are smaller by at least an order of magnitude. However, both the lower-mass spin-3/2 resonances $\Delta(1232)$ and $N(1520)$ give negative contributions to B_n, even though these states have different isospin and parity. On the other hand, the two higher-mass spin-3/2 states $\Delta(1700)$ and $N(1720)$, with opposite parity and different isospin, make positive contributions to the total B_n. No definite correlation between the isospin and parity is therefore observed in the imaginary part of the TPE amplitude for the case of normally polarized electrons elastically scattering from unpolarized protons.

At low beam energies the $\Delta(1232)$ state gives the dominant contribution to B_n, but as the energy increases, the higher-mass resonances start playing a more significant role. At $E_{\rm lab} = 0.855$ GeV, for example [Fig. 2(a)], the effect from the $N(1520)$, which has a nominal (*i.e.* zero-width) threshold energy $E_{\rm lab}^{\rm th} = 0.75$ GeV, becomes comparable to that of the $\Delta(1232)$. It is interesting to note that the higher-mass resonance states $\Delta(1700)$ and $N(1720)$ show non-negligible effects even at beam energies below their nominal excitation thresholds. However, at energies above threshold, the $\Delta(1700)$ and $N(1720)$ become important, as Figs. 2(b) demonstrates.

It is also important to note that at forward laboratory scattering angles $\theta_{\rm lab}$, where most of the experimental data exist, the $\Delta(1232)$ contribution alone is a good approximation to the total, with the small effects from other resonances largely canceling in this region. Furthermore, the elastic nucleon intermediate state gives a negligibly small effect in B_n, unlike the real part of the TPE amplitude in unpolarized ep elastic scattering [8].

The combined effect of all nine resonances, along with the nucleon elastic contribution, on the total B_n is illustrated in Fig. 3. At the lower beam energy $E_{\rm lab} = 0.855$ GeV, the overall B_n, including the effects of all elastic and resonance intermediate states, can be approximated by the $\Delta(1232)$ state alone. The total B_n remains negative over the entire range of scattering angles $\theta_{\rm lab}$. Compared with the experimental values, the calculated B_n overshoots the asymmetries measured by the A4 Collaboration at MAMI at $\theta_{\rm lab} \approx 35°$ [15, 20] [Fig. 3(a)]. On the other hand, the calculated

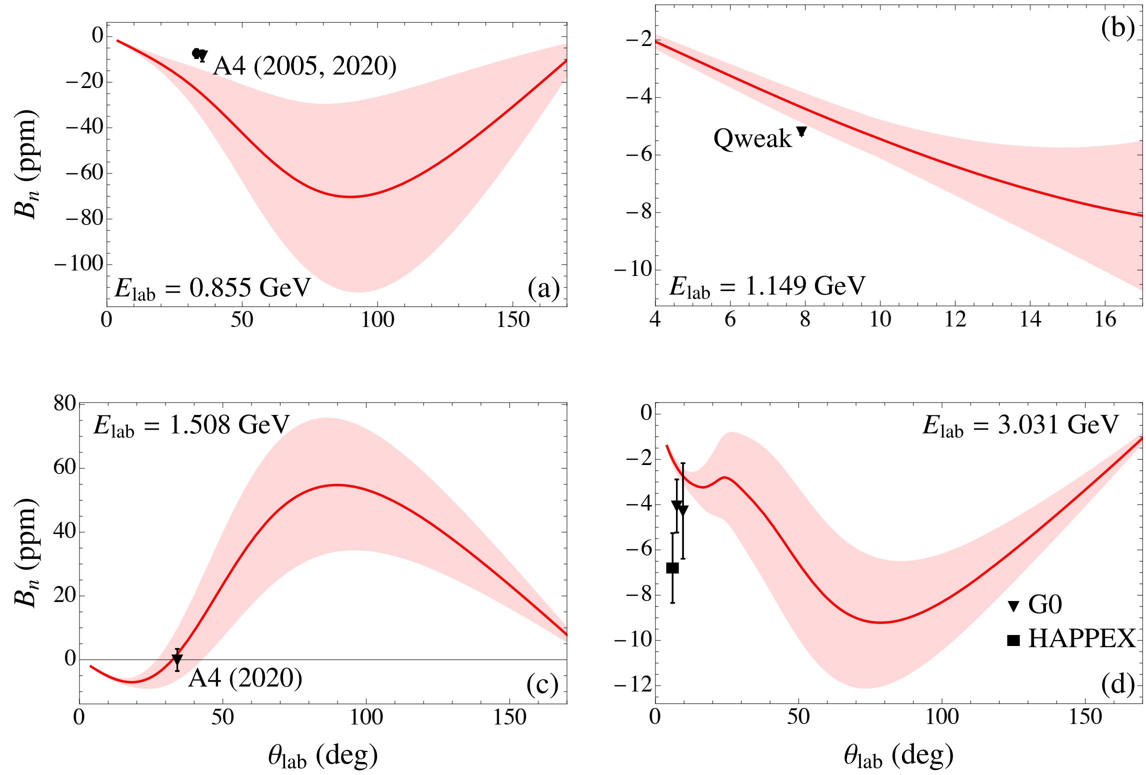

Figure 3: The total contribution from the nucleon elastic and all nine resonance states to the beam normal SSA B_n as a function of $\theta_{\rm lab}$ for fixed beam energies corresponding to the A4 [15, 20], $\mathrm{Q_{weak}}$ [21], G0 [16], and HAPPEX [18] experiments (black symbols).

B_n is in good agreement with the high-precision $\mathrm{Q_{weak}}$ measurement [21] at $E_{\rm lab} = 1.149$ GeV and $\theta_{\rm lab} = 7.9°$, within uncertainties [Fig. 3(b)]. Above $\theta_{\rm lab} = 30°$ B_n becomes large and positive (not shown), similar to the behaviour in Fig. 3(c).

The recent measurement of the asymmetry by the A4 Collaboration [20] at the larger beam energy $E_{\rm lab} = 1.508$ GeV and angle $\theta_{\rm lab} = 34.1°$ shows excellent agreement with the calculation. As seen in Fig. 3(c), the asymmetry changes sign to become positive at intermediate and backward scattering angles, $\theta_{\rm lab} \gtrsim 40°$ in the $E_{\rm lab} \approx 1-1.5$ GeV range (see also Fig. 4 below). At beam energy $E_{\rm lab} \approx 3$ GeV, three data points are available from the G0 [16] and HAPPEX [18] Collaborations in the forward angle region, $6° \leq \theta_{\rm lab} \lesssim 10°$. The calculated value of B_n agrees with the sign of the measured asymmetry within the uncertainty range, but has slightly smaller magnitude for the HAPPEX data point in particular.

To further illustrate the energy dependence of the total B_n, Fig. 4 shows the asymmetry as a function of $E_{\rm lab}$ up to 1.5 GeV at the two representative scattering angles $\theta_{\rm lab} = 35°$ and $145°$ that are close to the experimental values. Note again that at low energies the total asymmetry is dominated by the $\Delta(1232)$ state. Compared with the experimental data from the SAMPLE experiment [14] and the series of measurements by the A4 Collaboration [15, 19, 20], the calculations give the same sign as the data in Fig. 4 in the measured region. At the smaller scattering angle the calculation generally gives a larger magnitude for B_n than that observed, while at the larger scattering angles

PoS(SPIN2023)179

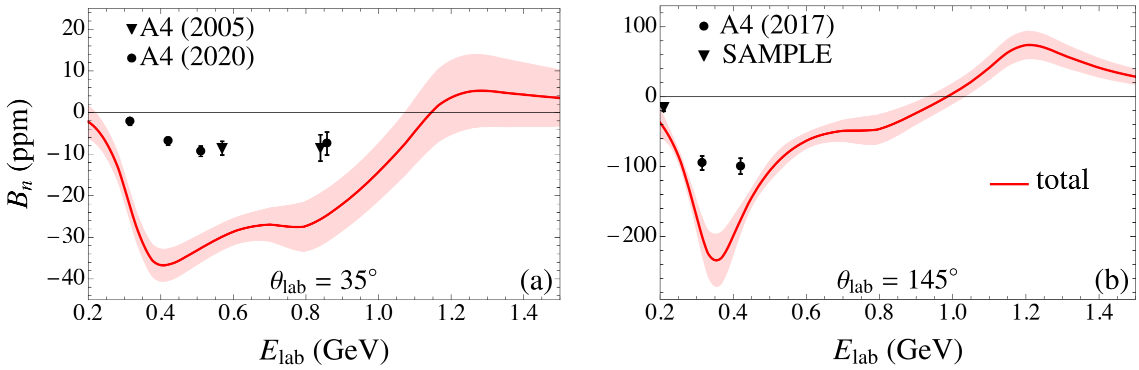

Figure 4: Beam normal SSA B_n as a function of beam energy E_{lab} in the lab frame at representative scattering angles $\theta_{\mathrm{lab}} = 35°$ and 145°. The total B_n is from the nucleon plus all nine resonances. The experimental data points in the forward angle region are from A4 experiments [15, 20], and in the backward angle region from the SAMPLE [14] and A4 [19] experiments.

the agreement between experiment and theory is reasonable, within uncertainties.

4. Conclusions

In this overview we have reported on beam normal single-spin asymmetries in elastic electron-proton scattering using the imaginary part of two-photon exchange amplitudes, including contributions from $J^P = 1/2^{\pm}$ and $3/2^{\pm}$ excited state resonances with mass below 1.8 GeV. Among the various intermediate state contributions to B_n, the elastic nucleon and spin 1/2 resonances are suppressed by an order of magnitude or more compared to the spin 3/2 resonances. The $\Delta(1232)$ resonance alone is a good approximation at forward angles for all beam energies. The $N(1520)$ contribution is noticeably smaller than the $\Delta(1232)$, but both are negative across the range of energies and angles considered. The $\Delta(1700)$ and $N(1720)$ are major contributors in the far forward and backward angle regions above their threshold excitation energies, both having positive contributions across energy and angle. As a result, the total B_n is somewhat sensitive to cancellations between the resonance contributions, changing from negative to positive with increasing energy and angle. Uncertainties in the input electrocouplings are also significant for the $N(1520)$, $\Delta(1700)$ and $N(1720)$ states, leading to a rather large overall uncertainty band in the total B_n.

The results reported in this work tend to overshoot the experimental B_n data at lower beam energies $E_{\mathrm{lab}} < 1$ GeV at both forward and backward angles. This is the region in which the $\Delta(1232)$ dominates, with relatively small uncertainties in its input parameters. There is good agreement between theory and the high-precision Qweak measurement at $E_{\mathrm{lab}} = 1.149$ GeV, and modest agreement at the highest available energy $E_{\mathrm{lab}} \sim 3$ GeV and very forward angles, where the experimental uncertainties from the G0 and HAPPEX data are rather large.

Acknowledgments

This work was supported by the Shahjalal University of Science and Technology Research Centre, the Natural Sciences and Engineering Research Council of Canada, and the US Department of Energy contract DE-AC05-06OR23177, under which Jefferson Science Associates, LLC operates Jefferson Lab.

References

[1] C.E. Carlson and M. Vanderhaeghen, *Two-Photon Physics in Hadronic Processes*, *Ann. Rev. Nucl. Part. Sci.* **57** (2007) 171 [hep-ph/0701272].

[2] J. Arrington, P.G. Blunden and W. Melnitchouk, *Review of two-photon exchange in electron scattering*, *Prog. Part. Nucl. Phys.* **66** (2011) 782 [1105.0951].

[3] A. Afanasev, P.G. Blunden, D. Hasell and B.A. Raue, *Two-photon exchange in elastic electron–proton scattering*, *Prog. Part. Nucl. Phys.* **95** (2017) 245 [1703.03874].

[4] D. Borisyuk and A. Kobushkin, *Two-Photon Exchange in Elastic Electron Scattering on Hadronic Systems*, *Ukr. J. Phys.* **66** (2021) 3 [1911.10956].

[5] P.A.M. Guichon and M. Vanderhaeghen, *How to reconcile the Rosenbluth and the polarization transfer method in the measurement of the proton form-factors*, *Phys. Rev. Lett.* **91** (2003) 142303 [hep-ph/0306007].

[6] P.G. Blunden, W. Melnitchouk and J.A. Tjon, *Two photon exchange and elastic electron proton scattering*, *Phys. Rev. Lett.* **91** (2003) 142304 [nucl-th/0306076].

[7] P.G. Blunden, W. Melnitchouk and J.A. Tjon, *Two-photon exchange in elastic electron-nucleon scattering*, *Phys. Rev. C* **72** (2005) 034612 [nucl-th/0506039].

[8] J. Ahmed, P.G. Blunden and W. Melnitchouk, *Two-photon exchange from intermediate state resonances in elastic electron-proton scattering*, *Phys. Rev. C* **102** (2020) 045205 [2006.12543].

[9] P.G. Blunden and W. Melnitchouk, *Dispersive approach to two-photon exchange in elastic electron-proton scattering*, *Phys. Rev. C* **95** (2017) 065209 [1703.06181].

[10] V.I. Mokeev, V.D. Burkert, T.-S.H. Lee, L. Elouadrhiri, G.V. Fedotov and B.S. Ishkhanov, *Model Analysis of the p pi+ pi- Electroproduction Reaction on the Proton*, *Phys. Rev. C* **80** (2009) 045212 [0809.4158].

[11] V.I. Mokeev et al., *Experimental Study of the $P_{11}(1440)$ and $D_{13}(1520)$ resonances from CLAS data on $ep \to e'\pi^+\pi^- p'$*, *Phys. Rev. C* **86** (2012) 035203 [1205.3948].

[12] A.N. Hiller Blin et al., *Nucleon resonance contributions to unpolarised inclusive electron scattering*, *Phys. Rev. C* **100** (2019) 035201 [1904.08016].

[13] A. De Rujula, J.M. Kaplan and E. De Rafael, *Elastic scattering of electrons from polarized protons and inelastic electron scattering experiments*, *Nucl. Phys.* **35** (1971) B365.

[14] S.P. Wells et al., *Measurement of the vector analyzing power in elastic electron proton scattering as a probe of double photon exchange amplitudes*, *Phys. Rev. C* **63** (2001) 064001 [nucl-ex/0002010].

[15] F.E. Maas et al., *Measurement of the transverse beam spin asymmetry in elastic electron proton scattering and the inelastic contribution to the imaginary part of the two-photon exchange amplitude*, *Phys. Rev. Lett.* **94** (2005) 082001 [nucl-ex/0410013].

[16] D.S. Armstrong et al., *Transverse Beam Spin Asymmetries in Forward-Angle Elastic Electron-Proton Scattering*, *Phys. Rev. Lett.* **99** (2007) 092301 [0705.1525].

[17] D. Androić et al., *Transverse Beam Spin Asymmetries at Backward Angles in Elastic Electron-Proton and Quasi-elastic Electron-Deuteron Scattering*, *Phys. Rev. Lett.* **107** (2011) 022501 [1103.3667].

[18] S. Abrahamyan et al., *New Measurements of the Transverse Beam Asymmetry for Elastic Electron Scattering from Selected Nuclei*, *Phys. Rev. Lett.* **109** (2012) 192501 [1208.6164].

[19] D.B. Ríos et al., *New Measurements of the Beam Normal Spin Asymmetries at Large Backward Angles with Hydrogen and Deuterium Targets*, *Phys. Rev. Lett.* **119** (2017) 012501.

[20] B. Gou et al., *Study of Two-Photon Exchange via the Beam Transverse Single Spin Asymmetry in Electron-Proton Elastic Scattering at Forward Angles over a Wide Energy Range*, *Phys. Rev. Lett.* **124** (2020) 122003 [2002.06252].

[21] D. Androić et al., *Precision Measurement of the Beam-Normal Single-Spin Asymmetry in Forward-Angle Elastic Electron-Proton Scattering*, *Phys. Rev. Lett.* **125** (2020) 112502 [2006.12435].

[22] J. Ahmed, P.G. Blunden and W. Melnitchouk, *Normal single-spin asymmetries in electron-proton scattering: Two-photon exchange with intermediate-state resonances*, *Phys. Rev. C* **108** (2023) 055202 [2306.02540].

[23] A.V. Afanasev and N.P. Merenkov, *Collinear photon exchange in the beam normal polarization asymmetry of elastic electron-proton scattering*, *Phys. Lett. B* **599** (2004) 48 [hep-ph/0407167].

[24] B. Pasquini and M. Vanderhaeghen, *Resonance estimates for single spin asymmetries in elastic electron-nucleon scattering*, *Phys. Rev. C* **70** (2004) 045206 [hep-ph/0405303].

[25] B. Pasquini and M. Vanderhaeghen, *Single spin asymmetries in elastic electron-nucleon scattering*, *Eur. Phys. J. A* **24S2** (2005) 29 [hep-ph/0502144].

[26] M. Gorchtein, *Beam normal spin asymmetry in the quasi-RCS approximation*, *Phys. Rev. C* **73** (2006) 055201 [hep-ph/0512105].

[27] J. Arrington, W. Melnitchouk and J.A. Tjon, *Global analysis of proton elastic form factor data with two-photon exchange corrections*, *Phys. Rev. C* **76** (2007) 035205 [0707.1861].